AJAB

Asian J Agric & Biol. 2024(1).
DOI: 10.35495/ajab.2023.144

Original Article

Transcriptome analysis of flower development and mining of genes related to the flower development in *Oncidium*

Nengyan Fang, Yuanhua Luo, Ronghui Fan, Xiuxian Ye, Minling Huang*, Huaiqin Zhong*
Institute of Crop Sciences, Fujian Academy of Agricultural Sciences (FAAS), Fujian Engineering Research Center of Characteristic Floriculture, Fuzhou, 350013 China

Received:
August 07, 2023
Accepted:
September 10, 2023
Published Online:
October 15, 2023

**Corresponding author email:*
zwshuahuizhongxin@163.com

Abstract

Oncidium, a kind of orchid plants characterized with unique flower, is one of the four tropical orchids with high ornamental value and favored by consumers. However, our understanding about the molecular basis of its flower development is still limited. Here, we collected *Oncidium* tissues at different developmental stages for RNA-seq. A total of more than 621 million clean reads were generated. 134,640 unigenes were assembled, and 54,221 unigenes were annotated. The number of DEGs (differentially expressed genes) was the largest in the comparison group F2-vs-F3 (F2 stage compared with F3 stage in flowers). The GO (Gene Ontology) terms and KEGG (Kyoto Encyclopedia of Genes and Genomes) pathways enriched for the specific DEGs were diverse at different stages. The common pathways enriched in multiple comparisons were also obtained. 11 key genes were obtained in cutin, suberin and wax biosynthesis pathway. Moreover, 32 candidate genes related to flower development were screened. Most of them presented tissue-specific expressions, especially MADS-box genes described by the ABCDE model. In all, the present data provides a valuable resource for dissecting the molecular mechanism of *Oncidium* in regulating flower development.

Keywords: Candidate genes, DEGs, Flower development, MADS-box genes, *Oncidium*, RNA-seq

How to cite this:

Fang N, Luo Y, Fan R, Ye X, Huang M and Zhong H. Transcriptome analysis of flower development and mining of genes related to the flower development in *Oncidium*. Asian J. Agric. Biol. 2024(1): 2023144. DOI: https://doi.org/10.35495/ajab.2023.144

Introduction

Orchidaceae is the largest and most widely distributed plant family with more than 25,000 species (Leitch et al., 2009). Among them, *Oncidium* is a large category, widely distributed in the Americas such as Mexico, Brazil, Bolivia and other tropical areas (Hew, 1992). It is one of the most important cut-flowers and potted flowers in the world. Its unique structure and beautiful colors are favored by consumers.

The flower of the dicotyledon model plant *Arabidopsis* has four whorls, and they are four sepals, four petals, six stamens and two carpels. The flower of rice, the model monocotyledon plant, also has the similar structure, and it consists of a pair of bract-like organs (lemma and palea), lodicules (equivalent to

eudicot petals), six stamens, and a carpel. Orchids have evolved into a unique group (Givnish et al., 2015). The structures of orchid flowers have unique diversifications, resulting from the long-term coevolution between insects and plants. The *Oncidium* has three sepals, two petals similar to sepals, a lip and a gynandrium that consists of an anther cap, two pollinium, a column, a carpel and an ovule. The lip, in particular, is an important organ that has evolved and is unique to *Oncidium*. Their unique flowers are so fascinating, and how they form is of great interest to researchers. Also, it is of great significance in *Oncidium* breeding to study the mechanism of the unique flower formation and mining of genes related to the flower development.

In plants, the MADS-box family genes play a critical role in flower developmental process (Callens et al., 2018). These genes can be divided into five classes (A, B, C, D and E), constituting the ABCDE model (Weigel and Meyerowitz, 1994; Theissen, 2001). The ABCDE model is generally conserved (Ferrario et al., 2004). In *Oncidium*, some MADS-box genes have been characterized to regulate the flower development. *OMADS10* is a putative *paleoAP1* (*paleoAPETALA1*) ortholog, and overexpression of *OMADS10* only causes moderately early flowering in transgenic *Arabidopsis* (Chang et al., 2009). *OMADS3*, *OMADS5* and *OMADS9* have been characterized as *AP3-like* (*APETALA3-like*) genes (Hsu and Yang, 2002). *OMADS5* can negatively affect lip formation (Chang et al., 2010). *OMADS8* has been characterized as *PI* (*PISTILLATA*) homolog, and it can cause the sepal into an expanded petal-like structure in transgenic *Arabidopsis* (Chang et al., 2010). *OMADS4* is characterized as *AG* (*AGAMOUS*) homolog, expressed in the reproductive organ column (Hsu et al., 2010). *OMADS2* is putative *STK-like* (*SEEDSTICK-like*) gene, expressed in the stigmatic cavity of column and ovary (Hsu et al., 2010). *OMADS6*, characterized as *SEP3* (*SEPALLATA 3*) homolog, and *OMADS11*, characterized as *SEP1/2* (*SEPALLATA 1/2*) homolog, regulate flower transition and formation (Hsu et al., 2003; Chang et al., 2009). *OMADS1* and *OMADS7* are characterized as *AGL6* (*AGAMOUS-like 6*) homologs, and their ectopic expressions can cause early flowering in *Arabidopsis* (Hsu et al., 2003; Chang et al., 2009).

The next-generation deep-sequencing technologies, such as Illumina RNA-sequencing (RNA-Seq) provide new approaches to study global transcriptome profiles for specific tissue research materials within a specific period (Marioni et al., 2008). In this study, RNA-Seq was performed on flowers, pseudobulbs, and leaves at different developmental stages using *Oncidium* variety Jihui. DEGs (Differentially expressed genes) were analyzed, GO (Gene Ontology) and KEGG (Kyoto Encyclopedia of Genes and Genomes) enriched were performed for the DEGs, and candidate genes related to the flower development were mined. The purpose was to provide theoretical support for studying the molecular mechanism of *Oncidium* flower regulation.

Material and Methods

Plant material

The *Oncidium* cultivar Jinhui was used in this study, an improved variety obtained from *Oncidium* Gower Ramsey (a hybrid from *Oncidium Goldiana* × *Oncidium Guiea* Gold). Three-year-old plants were grown in the greenhouse of the Institute of Crop Sciences, Fujian Academy of Agricultural Sciences (FAAS) (Fuzhou, China). Five developmental stages of the flower samples, floral meristem (F1), flower bud when septal and petal were green (F2), flower bud when septal and petal turned yellow (F3), flower bud before opening (F4), and mature flower (F5), were collected (Figure S1E). The leaf and pseudobulb samples were also collected from young, mature and flowering plants (Figure S1A-C). The pseudobulb (PB4) samples from post-flowering plants were also collected (Figure S1D). These samples were used for RNA extraction. Two independent RNA samples were used for each experiment in this study.

RNA extraction

Total RNA was extracted from collected samples with TRIzol kit (Invitrogen, Carlsbad, CA, USA) according to the manufacturer's instructions. RNA degradation and contamination were monitored on 1% agarose gels, and purity was checked using the NanoPhotometer® spectrophotometer (IMPLEN, CA, USA). RNA concentration was measured using the Qubit® RNA Assay Kit in the Qubit®2.0 Fluorometer (Life Technologies, CA, USA), and integrity was assessed using the RNA Nano 6000 Assay Kit of the Agilent Bioanalyzer 2100 system (Agilent Technologies, CA, USA).

cDNA library construction and Illumina sequencing

A total of 3 μg RNA per sample was used for the RNA

sample preparation, and twenty-four libraries were generated using the NEBNext®Ultra™ RNA Library Prep Kit for Illumina® (NEB, USA) following the manufacturer's recommendation. Briefly, after index codes added to attribute sequences to each sample, mRNA purified. Fragmentation was carried out using divalent cations under elevated temperature in NEBNext First Strand Synthesis Reaction Buffer (5X). First strand cDNA was synthesized using random hexamer primer and M-MuLV Reverse Transcriptase (RNase H Minus). Second strand cDNA synthesis was subsequently performed using DNA Polymerase I. After adenylation of 3' ends of DNA fragments, NEBNext Adaptor was ligated for hybridization. Then cDNA fragments of 150-200 bp in length were selected for PCR and the products were purified. After library quality assessed, the library preparations were sequenced on an Illumina Hiseq 2000 platform and paired-end reads were generated by Biomarker Inc. (Beijing, China). (NCBI SRA accession PRJNA532798).

Transcriptome assembly and gene annotation

Clean data were obtained by removing reads containing an adapter, reads containing ploy-N, and low-quality reads from raw data. Transcriptome assembly was accomplished using Trinity with min_kmer_cov set to 2, and all other parameters was set to default (Grabherr et al., 2011). The obtained unigenes were aligned against protein databases using blast software (Altschul et al., 1997) for function annotation, including the NCBI non redundant (Nr) protein database, Swiss-Prot (The UniProt Consortium, 2018), GO (Ashburner et al., 2000), COG (Clusters of Orthologous Groups) (Tatusov et al., 2000), KOG (euKaryotic Orthologous Groups) (Koonin et al., 2004), eggNOG4.5 (Huerta-Cepas et al., 2016), and KEGG (Kanehisa et al., 2004). The KEGG Orthology of Unigenes in KEGG was obtained using KOBAS 2.0 program (Xie et al., 2011). The E-value cutoff of Blast was set at 1e-5. After the amino acid sequence of UniGene was predicted, Hmmer software (Eddy, 1988) was used to compare with Pfam (Protein family) (Finn et al., 2014) database, and parameter E-value was set to < 1e-10.

Expression analysis of Unigenes

The sequenced reads were compared with Unigene library using Bowtie (Langmead et al., 2009). According to the comparison results, the expression level was estimated using RSEM (Li and Dewen, 2011). The FPKM (fragments per kilobase of transcript per million mapped reads) value indicated the gene expression level. The average FPKM of unigene <= 1.0 was identified as not expressed.

The differential expression analysis was performed using the DESeq (Anders and Huber, 2010). DESeq provided statistical analysis for determining differential expressions in the DGEs, using a model based on the negative binomial distribution. The resulting *P*-values were adjusted using the Benjamini-Hochberg approach to control the false discovery rate (FDR). Genes with an adjusted *P*-value < 0.01 of FDR and fold change (FC) >= 2 obtained by DESeq were assigned as differentially expressed. FC represented the ratio of expression between two groups.

Phylogenetic analysis of MADS-box genes

The MADS-box family protein sequences of *Arabidopsis* were obtained from the *Arabidopsis* Information Resource (TAIR, http://www.Arabidopsis.org/), and the MADS-box family protein sequences of rice (*Oryza sativa*) were downloaded from the Rice Genome Annotation Project (http://rice.uga.edu/). The MADS domains were analyzed using SMART (http://smart.embl-heidelberg.de/). The MADS-box protein domain sequences of *Arabidopsis*, rice and *Oncidium* were aligned using ClustalW program. A neighbor-joining (NJ) phylogenetic tree was constructed using MEGAX64 with default parameters, and the bootstrap analysis was set at 1000 replicates.

Quantitative real-time PCR (qRT-PCR) analysis

To validate the accuracy of the transcriptome profile, total RNA was extracted from samples using the TRIzol kit. The total RNA was reverse transcribed into cDNA using the PrimeScript™ 1st Strand cDNA Synthesis Kit (TaKaRa, Dalian, China), according to the manufacturer's protocol. Nine unigenes were selected for evaluation by qRT-PCR, using ABI 7500 Real Time System and SYBR GREEN PCR Master Mix (TaKaRa, Dalian, China). The primers were listed in Table - -S1. Actin was used as an internal control. Reactions were performed at 94 °C for 2 min, then cycled at 95 °C for 30 s, 48-54 °C for 30 s, 72 °C for 30 s for 35 cycles, and finally, 72 °C for 10 min. Each assay was performed in triplicate. Data analysis was performed using the $2^{-\Delta\Delta Ct}$ method (Livak and Schmittgen, 2001).

Results

Illumina sequencing and sequence assembly

In this study, 621,709,321 clean reads were generated with an average length of 295 bp. The average percentages of GC and Q30 were 46.78% and 91.87%, respectively. After assembly, 134,640 unigenes were obtained with an average length of 954 bp and an N50 of 1,445 bp (Table - -1). 31.90% of unigenes were >= 1000 bp in length, and the length distribution of unigenes was shown in Figure S2.

Table-1. Summary for *Oncidium* transcriptome

Items	Value
Total number of clean reads	621,709,321
Total clean nucleotides (nt)	183,534,969,996
Average read length (bp)	295
GC (%)	46.78
Q30 (%)	91.87
Total number of unigenes	134,640
Mean length of unigenes (bp)	954
N50 length (bp)	1,445

Notes: Q30 means the probability of base recognition error is 0.1%, or the accuracy rate is 99.9%. N50 means the shortest contig length obtained when the cumulative length of the longest contig length equals 50% of the total assembly length.

Gene annotation and functional classification

In total, 54,221 (40.27%) of the assembled unigenes could be annotated (Table - S2). 53,393 (39.66%) unigenes hit with the Nr databases. 53.38% of the matches presented 60% or more similarity. In a subsequent gene matching analysis, the dominant closest matches included *Elaeis guineensis* (25.74%), *Phoenix dactylifera* (22.17%) and *Musa acuminate subsp. Malaccensis* (9.74%) (Figure S3BC). The Blast Nr E-value distribution was showed in Figure S3A.

Totally 32,768 (24.34%) and 35,910 (26.67%) unigenes hit with the Swiss-Prot and Pfam databases, respectively. 15,061 (11.19%), 31,664 (23.52%) and 49,772 (36.97%) unigenes were classified into 25 function classifications in the COG, KOG, and eggNOG, respectively (Figure S4). The largest group was 'general function prediction only' in KOG and eggNOG classification. While in COG classification, the cluster 'replication, recombination, and repair' represented the largest group, followed by 'general function prediction only'.

In GO classification, 28,872 (21.44%) unigenes were categorized into three main groups and 53 sub-functional groups (Figure S5). Dominant cellular component categories were included 'nucleoid', 'cell part' and 'organelle'. The primarily molecular function categories included 'catalytic activity', 'binding' and 'transporter activity'. 15,697 (11.66%) unigenes were mapped to the KEGG database, and 126 biochemical pathways were obtained (Table - S3). 'Ribosome pathway' presented the largest number of unigenes, followed by 'carbon metabolism', and 'biosynthesis of amino acids'.

Differentially expressed genes analysis in flower

Comparisons were performed between DEG libraries at adjacent stages. A total of 2,251 DEGs were detected in F1-vs-F2, with 1,599 genes up-regulated and 652 genes down-regulated. In F2-vs-F3, the largest number of DEGs (5,159) was identified, with 1,889 genes up-regulated and 3,270 genes down-regulated. In the F3-vs-F4, the fewest number of DEGs (1,317) was identified, with 574 genes up-regulated and 743 genes down-regulated. There were 1,846 DEGs detected in F4-vs-F5, with 725 genes up-regualed and 1,211 genes down-regulated (Figure 1A). The results showed that DEGs were the most active during the flower development from F2 to F3 stage.

The specific DEGs uniquely detected at different stages were analyzed. The Venn diagram of the DEGs showed the number of DEGs only identified in each comparison groups and the overlap relationship between the comparison groups. The largest number of the specific DEGs was detected only in the F2-vs-F3, with 1,491 genes up-regulated and 2,924 genes down-regulated. There were three common up-regulated DEGs shared by all four comparisons, and these genes might be closely related to the regulation of the flower development (Figure 1B). They were *alternative oxidase 1* (*BMK_Unigene_023270*), *ubiquinol oxidase 2* (*BMK_Unigene_023271*) and *CER4* (*ECERIFERUM 4*) (*BMK_Unigene_112129*).

GO and KEGG enrichment analysis of the specific DEGs

In order to analyze the developmental characteristics of flowers at different stages, the GO-term enrichment analysis was performed on the specific DEGs that were uniquely detected in different comparisons. The results revealed that the GO terms

enriched at different stages were diverse. The GO terms for the specific up-regulated and down-regulated DEGs were mainly enriched in biological process and molecular function (Figure S6).

For the specific up-regulated DEGs, several categories possibly associated with the flower development were found, including 'cutin biosynthetic process', 'trehalose biosynthetic process' and 'sporopollenin biosynthetic process' in F1-vs-F2, 'chitinase activity' and 'chitin catabolic process' in F2-vs-F3, 'terpene synthase activity' and 'polar nucleus fusion' in F3-vs-F4, and 'carotene catabolic process' in F4-vs-F5. Different categories were enriched for the specific down-regulated DEGs, and categories possibly associated with the flower development also were found, such as 'flower morphogenesis' and 'floral whorl development' in F1-vs-F2, 'floral organ development' and 'reproductive process' in F2-vs-F3, 'cutin biosynthetic process' and 'fatty acid biosynthetic process' in F3-vs-F4, and 'carbohydrate metabolic process' in F4-vs-F5.

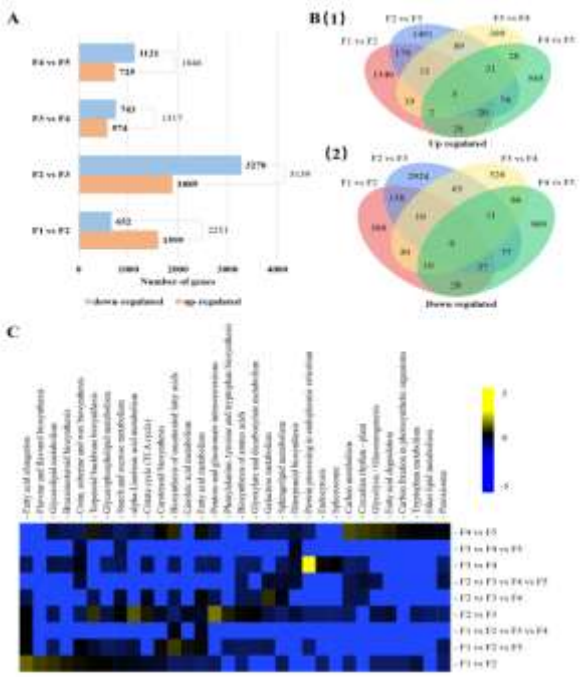

Figure-1. DEGs detected in flowers and annotation. A. Numbers of DEGs in each comparison in flowers. B. Venn diagrams of DEGs in comparisons. (1) Venn diagrams of up-regulated DEGs in comparisons. (2) Venn diagrams of down-regulated DEGs in comparisons. C. KEGG pathways enriched for specific up-regulated DEGs in each comparison in flowers. -Log_{10} $^{(100*p\_value)}$ was used to plot the heatmap. Yellow indicated low *p*-value and blue indicated high *p*-value.

KEGG analysis were performed on the specific up-regulated DEGs in different comparisons. The results (P <= 0.01) showed that 32 biochemical pathways were obtained (Figure 1C). Most of the specific up-regulated genes in each combination were significantly enriched in different pathways. 'Flavone and flavonol biosynthesis', 'glycerolipid metabolism', 'brassinosteroid biosynthesis' and 'glycerophospholipid metabolism' pathways were only significantly enriched in the F1-vs-F2. Seven pathways were only significantly enriched in the F2-vs-F3, such as 'starch and sucrose metabolism', 'alpha-linolenic acid metabolism', 'citrate cycle (TCA cycle), etc. The fewest number of the specific pathways were significantly enriched in the F3-vs-F4, including 'protein processing in endoplasmic reticulum', 'endocytosis' and 'spliceosome'. While the largest number of the specific pathways were significantly enriched in the F4-vs-F5, including eight pathways such as 'carbon metabolism', 'circadian rhythm - plant', 'glycolysis/gluconeogenesis', etc. The common pathways enriched in multiple comparisons were obtained, including 'fatty acid elongation', 'cutin, suberine and wax biosynthesis', 'carotenoid biosynthesis', 'biosynthesis of unsaturated fatty acids', 'terpenoid backbone biosynthesis', 'biosynthesis of unsaturated fatty acids', 'fatty acid metabolism', 'galactose metabolism', and 'sphingolipid metabolism'.

Analysis of genes related to flower development

Based on gene expression, GO description, KEGG pathway description, and combined with related references, 32 candidate genes related to flower development were screened (Table - 2, Table - S4). The largest number of them is MADS-box gene. The phylogenetic analysis was performed using the MADS conserved domain of MADS-box genes, including the related MADS-box genes in *Oncidium*, rice and *Arabidopsis* (Arora et al., 2007). The result showed that MADS-box candidate genes in *Oncidium* included *STK*, *AG*, two *AP1* homologs, two *AP3* homologs, *AGL6*, two *AGL12* (*AGAMOUS-like 12*) homologs, *AGL65* (*AGAMOUS-like 65*), *SEP1*, *SEP2* and *SVP* (*SHORT VEGATATIVE PHASE*) (Figure 2A). Among them, some genes were found the corresponding genes that had characterized in *Oncidium*, such as *AP1* (*BMK_Unigene_026197*), two *AP3* homologs and *SEP1*. While *BMK_Unigene_020766* (*AP1*) and *OMADS10*,

BMK_Unigene_034758 (*AG*) and *OMADS4*, and *BMK_Unigene_004701* (*AGL6*) and *OMADS1* were clustered into the different branches respectively, suggesting that they probably were different genes. Some genes had not been characterized in *Oncidium* yet, such as *SEP2*, *SVP*, *AGL12* and *AGL65*.

It seemed that most of MADS-box genes described by the ABCDE model were preferentially expressed in flowers. *BMK_Unigene_020766* (*AP1*) was mainly expressed in vegetative tissues and less in flowers. In addition to being highly expressed in vegetative tissues, *BMK_Unigene_026197* (*AP1*) is also relatively expressed at F1, F4 and F5 stages. Two *AP3* homologs (*BMK_Unigene_038423* and *BMK_Unigene_118517*) were expressed in flowers at different stages. While the expression of *BMK_Unigene_038423* (*AP3*) was also both detected in pseudobulbs and leaves. The expressions of *BMK_Unigene_034758* (*AG*) and *BMK_Unigene_042575* (*STK*) were only detected in flowers. While the expression of *BMK_Unigene_034758* (*AG*) was barely detected in flower buds at F1 and F3 stages. *BMK_Unigene_040222* (*SEP1*) and *BMK_Unigene_029684* (*SEP2*) were expressed in flowers at different stages. The expression of *BMK_Unigene_040222* (*SEP1*) was also detected in young pseudobulbs. *BMK_Unigene_004701* (*AGL6*) was expressed in flowers at different stages and in leaves at L1 and L3 stages. *BMK_Unigene_113329* (*AGL12*) and *BMK_Unigene_117532* (*AGL65*) were mainly expressed in flowers. While *BMK_Unigene_042320* (*AGL12*) and *BMK_Unigene_041872* (*SVP*) were mainly expressed in vegetative tissues (Figure 2B).

Six genes regulating flowering time, *FKF1* (*FLAVIN-BINDING, KELCH REPEAT, and F-BOX 1*), *FLK* (*FLOWERING LOCUS WITH KH DOMAINS*), *GI* (*GIGANTEA*), *HY5* (*Elongated hypocotyl 5*), *ICU2* (*INCURVATA2*) and *MET1* (*methyltransferase 1*), were screened. *GI* and *HY5* were all expressed in flowers, pseudobulbs and leaves. *FLK* was not expressed in young leaves. *FKF1* was not expressed in flower buds at F4 stage. *ICU2* was mainly expressed in flower buds and young pseudobulbs. *MET1* was only expressed in flowers at F1 and F2 stages. Four genes related to inflorescence development, *AGO1* (*ARGONAUTE 1*), *AIM1* and two *CORYNE* homologs, were screened. *AGO1* was only expressed in flowers. *AIM1* was expressed in flower buds and young pseudobulbs. The expressions of two *CORYNE* homologs were detected in flowers, pseudobulbs and young leaves. *ACLA-2* (*ATP-citrate lyase A-2*), *AMP1* (*ALTERED MERISTEM PROGRAM 1*), *ARF5* (*AUXIN RESPONSE FACTOR 2*), *GPAT6* (*glycerol-3-phosphate acyltransferase 6*), *HK2* (*histidine kinase 2*), *TAR2* (*TRYPTOPHAN AMINOTRANSFERASE RELATED 2*) and *TGA8* (*TGACG sequence-specific binding protein 8*) were thought to be involved in floral organ development. *ARF5* and *TGA8* were only expressed in flowers at F1, F2 and F3 stages, and the expressions were the highest in flowers at F1 stage. *ACLA-2* (*BMK_Unigene_017726*), *HK2* and two *GPAT6* homologs were expressed both in flowers and vegetative tissues at different stages. While *ACLA-2* (*BMK_Unigene_089599*) was only expressed in flowers and young pseudobulbs. The expression of *FLK* could not be detected in young leaves. The expression of *TAR2* could not be detected in pseudobulbs of young, mature and post-flowering plants (Figure 2B).

Table-2. Flower development-related genes in *Oncidium*

Gene ID	Gene Symbol	GeneBank Description	Accession	E value
BMK_Unigene_017726	ACLA-2	ATP-citrate lyase A-2 [*Arabidopsis thaliana*]	NP_001320572.1	0
BMK_Unigene_089599	ACLA-2	ATP-citrate lyase A-2 [*Arabidopsis thaliana*]	NP_001320572.1	0
BMK_Unigene_033489	AGO1	Stabilizer of iron transporter SufD / Polynucleotidyl transferase [*Arabidopsis thaliana*]	NP_001185169.1	0
BMK_Unigene_063492	AIM1	Enoyl-CoA hydratase/isomerase family [*Arabidopsis thaliana*]	NP_194630.1	0
BMK_Unigene_018210	AMP1	Peptidase M28 family protein [*Arabidopsis thaliana*]	NP_567007.1	0
BMK_Unigene_049059	ARF5	Transcriptional factor B3 family protein / auxin-responsive factor AUX/IAA-like protein [*Arabidopsis thaliana*]	NP_173414.1	0
BMK_Unigene_087654	CORYNE	Protein kinase superfamily protein [*Arabidopsis thaliana*]	NP_850812.2	1.00E-130
BMK_Unigene_119565	CORYNE	Protein kinase superfamily protein [*Arabidopsis thaliana*]	NP_850812.2	7.00E-135
BMK_Unigene_089905	FKF1	Flavin-binding, kelch repeat, f box 1 [*Arabidopsis thaliana*]	NP_564919.1	0
BMK_Unigene_122609	FLK	RNA-binding KH domain-containing protein [*Arabidopsis thaliana*]	NP_001325772.1	3.00E-10
BMK_Unigene_050492	GI	GIGANTEA [*Arabidopsis thaliana*]	NP_564180.1	0
BMK_Unigene_042209	GPAT6	Glycerol-3-phosphate acyltransferase 6 [*Arabidopsis thaliana*]	NP_181346.1	1.00E-104
BMK_Unigene_048418	GPAT6	Glycerol-3-phosphate acyltransferase 6 [*Arabidopsis thaliana*]	NP_181346.1	0
BMK_Unigene_008170	HK2	Histidine kinase 2 [Arabidopsis thaliana]	NP_568532.1	0
BMK_Unigene_018187	HY5	Basic-leucine zipper (bZIP) transcription factor family protein [*Arabidopsis thaliana*]	NP_568246.1	4.00E-43
BMK_Unigene_014851	ICU2	DNA-directed DNA polymerase; INCURVATA2 [*Arabidopsis thaliana*]	NP_001331725.1	0
BMK_Unigene_013169	MET1	Methyltransferase 1 [*Arabidopsis thaliana*]	NP_199727.1	0
BMK_Unigene_032233	TAR2	Tryptophan aminotransferase related 2 [*Arabidopsis thaliana*]	NP_567706.1	1.00E-147
BMK_Unigene_004530	TGA8	PERIANTHIA (PAN); TGACG sequence-specific binding protein 8 (TGA8) [*Arabidopsis thaliana*]	NP_177031.1	6.00E-136
BMK_Unigene_034758	AG	AGAMOUS [*Arabidopsis thaliana*]	NP_567569.3	4E-87
BMK_Unigene_042575	STK	AGAMOUS [*Arabidopsis thaliana*]	NP_567569.3	7E-96
BMK_Unigene_004701	AGL6	AGAMOUS-like 6 [*Arabidopsis thaliana*]	NP_182089.1	4E-32
BMK_Unigene_042320	AGL12	AGAMOUS-like 12 [*Arabidopsis thaliana*]	NP_565022.1	9E-42
BMK_Unigene_113329	AGL12	AGAMOUS-like 12 [*Arabidopsis thaliana*]	NP_565022.1	6E-43
BMK_Unigene_117532	AGL65	AGAMOUS-like 65 [*Arabidopsis thaliana*]	NP_001321506.1	4E-77
BMK_Unigene_020766	AP1	AGAMOUS-like 8; APETALA1; FUL [*Arabidopsis thaliana*]	NP_568929.1	3E-81
BMK_Unigene_026197	AP1	AGAMOUS-like 7; APETALA1 [*Arabidopsis thaliana*]	NP_001320362.1	3E-79
BMK_Unigene_038423	AP3	APETALA3 [*Arabidopsis thaliana*]	NP_191002.1	6E-64
BMK_Unigene_118517	AP3	APETALA3 [*Arabidopsis thaliana*]	NP_191002.1	3E-66
BMK_Unigene_040222	SEP1	AGAMOUS-like 2; SEPALLATA1 [*Arabidopsis thaliana*]	NP_568322.1	3E-100
BMK_Unigene_029684	SEP2	AGAMOUS-like 4; SEPALLATA 2 [*Arabidopsis thaliana*]	NP_186880.1	3E-91
BMK_Unigene_041872	SVP	AGAMOUS-like 22; SHORT VEGATATIVE PHASE [*Arabidopsis thaliana*]	NP_001324584.1	1E-77

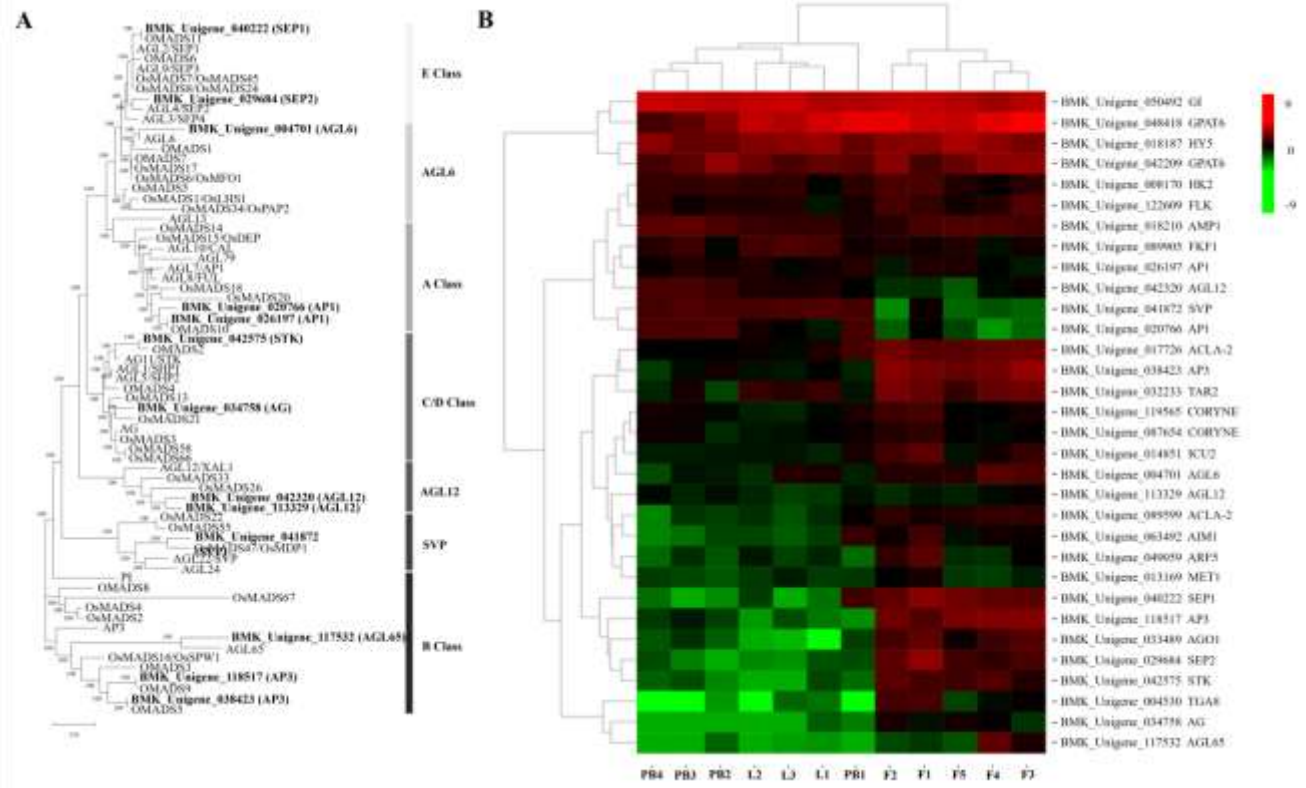

Figure-2. Genes related to the flower development. A. Phylogenetic tree of MADS-box genes in Arabidopsis, rice and *Oncidium*. OMADS1-10 have been characteried in previous researches. All the MADS-box protein domain sequences were aligned using ClustalW program. The neighbor-joining tree was constructed using MEGAX64 program with bootstrap analysis of 1000 replicates. The branch length represented the distance length. The number represented the percent of data coverage for inter notes. B. Heatmap and clustering diagram showing the expression patterns of 32 candidate genes related to the flower development in different tissues. Log2-transformed FPKM values were used to plot the heatmap. The color scale indicated gene expression. Red indicated high expression, and green indicated low expression.

Analysis of genes related to cutin biosynthesis

The morphology of floral surfaces depends on the synthesis of cutin (Li-Beisson et al., 2009). In this study, the cutin, suberine and wax biosynthesis as a common pathway was enriched in multiple comparisons. 11 genes were screened in this pathway, including *ACE*/*HTH* (*ADHESION OF CALYX EDGES/HOTHEAD*), *CYP86A1*, *CYP86A4*, four *CER1* (*ECERIFERUM 1*) homologs, two *FAR1* (*alcohol-forming fatty acyl-CoA reductase 1*) homologs and two *FAR4* (*alcohol-forming fatty acyl-CoA reductase 4*) homologs (Table - 3, Figure 3). The expression of *ACE*/*HTH* was detected in flowers, pseudobulbs and leaves, and the expression in flowers was higher than other tissues. *CYP86A1* was expressed in flowers at different stages, pseudobulbs of young and mature plants and young leaves. *CYP86A4* had a similar expression pattern to that of *CYP86A1*. Four *CER1* homologs had different expression patterns. The expression of *BMK_Unigene_120875* (*CER1*) was only detected in flowers, while the expression of *BMK_Unigene_045810* (*CER1*) was detected in all tissues. *BMK_Unigene_001977* (*CER1*) had a similar expression pattern to *BMK_Unigene_045810* (*CER1*), except for that in pseudobulbs of the post-flowering plants. *BMK_Unigene_054532* (*CER1*) was expressed mainly in flowers and certain vegetative tissues. *FAR1* (*BMK_Unigene_029767* and *BMK_Unigene_082189*) had same expression

patterns. Their expressions were detected in flowers and young pseudobulbs, and showed up-regulated in flowers with the flower development. *BMK_Unigene_029767* (*FAR4*) was only expressed in flowers at F3, F4 and F5 stages. *BMK_Unigene_082189* (*FAR4*) was only expressed in flowers at F4 and F5 stages. The expressions of both two *FAR4* homologs showed up-regulated with the flower development.

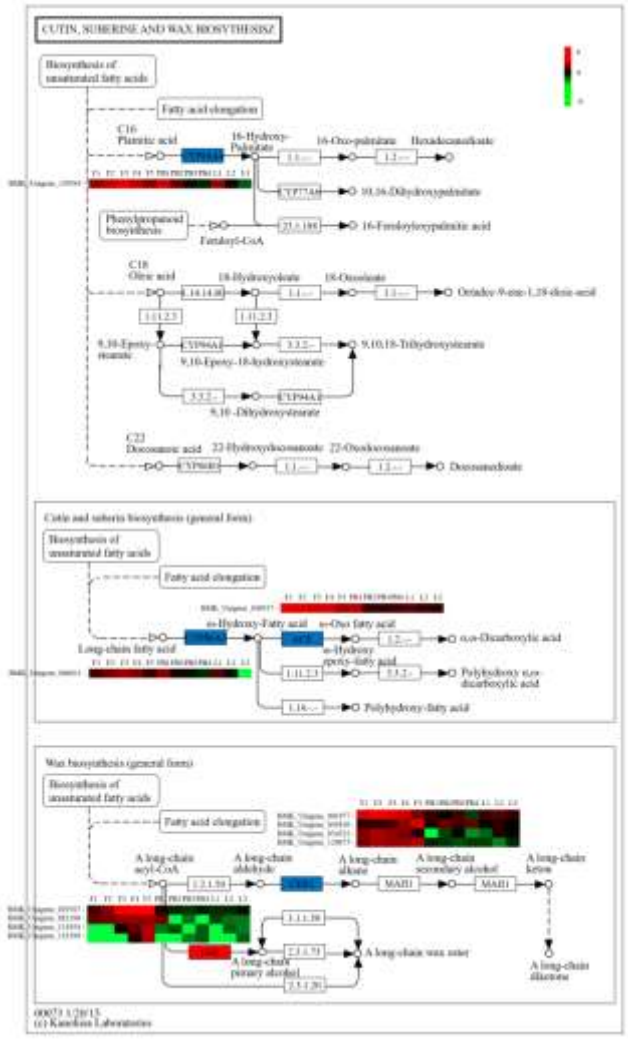

Figure-3. Regulatory changes in the pathway of cutin, suberin and wax biosynthesis during the flower development. Colored boxes, genes identified in our data; blue boxes, mixed regulated genes in different satges; red boxes, up-regulated genes; dark blue boxes, down-regulated genes. Log2-transformed FPKM values were used to plot the heatmap. The color scale presents gene expression, where red indicates high expression and green indicates low expression.

Table-3. Genes involving cutin suberine and wax biosynthesis

Gene ID	Gene Symbol	GeneBank Description	Accession	E value
BMK_Unigene_066611	CYP86A1	CYP86A1 [*Arabidopsis thaliana*]	NP_200694.1	4.00E-47
BMK_Unigene_129345	CYP86A4	CYP86A4 [*Arabidopsis thaliana*]	NP_171666.1	2.00E-60
BMK_Unigene_049557	ACE	ACE [*Arabidopsis thaliana*]	NP_565050.1	0
BMK_Unigene_001977	CER1	CER1 protein [*Arabidopsis thaliana*]	NP_001320547.1	9.00E-101
BMK_Unigene_045810	CER1	CER1 protein [*Arabidopsis thaliana*]	NP_171723.2	8.00E-96
BMK_Unigene_054532	CER1	CER1 protein [*Arabidopsis thaliana*]	NP_001320548.1	3.00E-105
BMK_Unigene_120875	CER1	CER1 protein [*Arabidopsis thaliana*]	NP_001320548.1	1.00E-84
BMK_Unigene_029767	FAR1	FAR1 [*Arabidopsis thaliana*]	NP_001331256.1	3.00E-145
BMK_Unigene_082189	FAR1	FAR1 [*Arabidopsis thaliana*]	NP_197642.1	1.00E-39
BMK_Unigene_131954	FAR4	FAR4 [*Arabidopsis thaliana*]	NP_190040.3	5.00E-35
BMK_Unigene_133398	FAR4	FAR4 [*Arabidopsis thaliana*]	NP_190040.3	2.00E-36

qRT-PCR validation

To validate the gene expression levels obtained from Illumina RNA-Seq results, nine unigenes including two *AP1*, two *AP3*, *AG*, *STK*, *SEP1*, *SEP2* and *AGL6*, were selected for real-time PCR analysis. The results showed that *AP3*, *AG*, *STK*, *SEP1*, *SEP2* and *AGL6* were mainly expressed in flowers, and displayed lower expression level in vegetative tissues. While *BMK_Unigene_020766* (*AP1*) and *BMK_Unigene_026197* (*AP1*) was mainly expressed in leaves and pseudobulbs, and *BMK_Unigene_020766* (*AP1*) displayed higher expression level in pseudobulbs than that in leaves. Overall, the expression patterns of these nine genes were consistent with the RNA-Seq assay, verifying the reliability of the Illumina sequencing data (Figure S7).

Discussion

Currently, there are few available genomic information of *Oncidium* that can provide insights into the mechanisms behind the flower development. In this study, a large number of cDNA sequencing data were generated, facilitating the identification of genes regulating the flower development in

Oncidium. A set of 621 million clean reads were generated, and assembled into 134,640 unigenes. After annotation against protein databases, we concluded that 40.27% of unigenes were annotated as putative functions and > 50% of unigenes had no homologs in the databases used. These transcriptome data provided us more and novel unigenes to predict the flower development in *Oncidium.*

A limited number of MADS-box genes have been characterized in *Oncidium*. In A class, *AP1*/*FUL* is required for establishment of the floral meristem (Mandel et al., 1992). In *Oncidium*, *OMADS10* is characterized as a putative *AP1* ortholog, and is expressed in lip, carpel/ovule of flowers and leaves (Chang et al., 2009). In this study, Two *AP1* homologs (*BMK_Unigene_020766* and *BMK_Unigene_026197*) were obtained. *BMK_Unigene_026197* was expressed in floral meristems, mature flowers and vegetative tissues, similar to the expression pattern of *OMADS10* (Chang et al., 2009). Based on the phylogenetic analysis and expression results, it was inferred that *BMK_Unigene_026197* probably was *OMADS10*. While *BMK_Unigene_020766* had a different expression pattern, with high expression in vegetative tissues rather than in flowers. The phylogenetic analysis result showed that *BMK_Unigene_020766* placed different branch with *OMADS10*. The results suggested that *BMK_Unigene_020766* was different form *OMADS10*, and there were at least two genes in A class in *Oncidium*. *BMK_Unigene_020766* probably had a different function in regulating the flower development. In class B, *OMADS3*, *OMADS5* and *OMADS9* have been characterized as *AP3-like* genes in previous studies (Chang et al., 2010). *OMADS8* has been characterized as *PI* homolog (Chang et al., 2010). *OMADS3* and *OMADS8* are expressed in floral organs as well as in vegetative leaves. *OMADS5* and *OMADS9* are strongly expressed in sepal and petal of flowers (Chang et al., 2010). In this study, only two *AP3* homologs (*BMK_Unigene_038423* and *BMK_Unigene_118517*) were obtained. Their expression patterns are similar to those of *OMADS5* and *OMADS9*, and they are mainly expressed in flowers. The phylogenetic analysis result showed that *BMK_Unigene_038423* and *OMADS5*, *BMK_Unigene_118517* and *OMADS9* were clustered in the same branch, respectively. The results suggested that *BMK_Unigene_038423* probably was *OMADS5* and *BMK_Unigene_118517* probably was *OMADS9*. No *PI* homologs were obtained in this study. In C class, *AG* is required for determinacy of stamen and carpel development (Yanofsky et al., 1990). *OMADS4* is characterized as *AG* homolog, and is expressed in the reproductive organ column (Hsu et al., 2010). In this study, *BMK_Unigene_034758* was characterized as *AG* homolog, and its expression was mainly detected in flowers at F2, F4 and F5 stages. The phylogenetic analysis result showed that *BMK_Unigene_034758* and *OMADS4* were clustered into different branches, and their genetic relationship was relatively distant. The results suggested that *BMK_Unigene_034758* and *OMADS4* were different genes, and there were at least two C class genes in *Oncidium*. In D class, *OMADS2* is putative *STK-like* gene, and is expressed in the stigmatic cavity of column and ovary (Hsu et al., 2010). In this study, *BMK_Unigene_042575* was characterized as *STK* homolog. *BMK_Unigene_042575* was only expressed in flowers. There was a certain distance between *BMK_Unigene_042575* and *OMADS2* in the phylogenetic tree, suggesting that they were different genes. The results showed that there were at least two genes in D class in *Oncidium*. In E class, *OMADS6* as *SEP3* homolog, and *OMADS11* as *SEP1/2* homolog have been characterized, and they are expressed in flowers and but not in leaves (Hsu et al., 2003; Chang et al., 2009). *BMK_Unigene_040222* was characterized as *SEP1*. The phylogenetic analysis result showed that *BMK_Unigene_040222* and *OMADS11* were clustered in the same branch, and their expression patterns were the same, indicating that *BMK_Unigene_040222* probably was *OMADS11*. *BMK_Unigene_029684* was characterized as *SEP2* homolog, and its expression pattern in flowers was different from that of *BMK_Unigene_040222*, suggesting that it exhibited different roles in regulating the flower development. *SEP3* homolog and *SEP4* homolog were not found in this study. *OMADS1* and *OMADS7* have been characterized as *AGL6* homologs, and their expressions could be detected in floral organs, but not in leaves (Hsu et al., 2003; Chang et al., 2009). In this study, *BMK_Unigene_004701* was characterized as *AGL6* homolog. *BMK_Unigene_004701* was expressed in both flowers and leaves, which was different from the expression patterns of *OMADS1* and *OMADS7*. In addition, the phylogenetic analysis result showed that *BMK_Unigene_004701*, *OMADS1* and *OMADS7* were not clustered into the same

branch. The results suggested that *BMK_Unigene_004701* was not *OMADS1* or *OMADS7*. In all, the pattern of these MADS-box genes we inferred regulating the flower development of *Oncidium* was shown in the Figure S8.

In addition to MADS-box genes, genes regulating flowering time were obtained, such as *GI*, *FKF1* and *HY5* in photoperiod pathway, *SVP* in ambient temperature pathway, *ICU2* in vernalization pathway, and *FLK* in the autonomous pathway. *GI* and *FKF1* are related to the circadian rhythm. They can form a complex and promote the expression of *CO* (*CONSTANS*), thus regulating the flowering time of plants (Imaizumi et al., 2005; Sawa et al., 2007). HY5 can bound directly to the promoter regions of *PIF4* (*PHYTOCHROME-INTERACTING FACTOR 4*) and *COL5* (*CONSTANS-LIKE 5*), and then represses their expressions, varying flowering time in *Arabidopsis* (Chu et al., 2022). *GI*, *FKF1* and *HY5* were expressed in flowers, pseudobulbs and leaves of *Oncidium* at different stages, but their expression patterns were different. The expression level of *GI* in *Oncidium* leaves and pseudobulbs increased with the growth of *Oncidium*, while the expression level in flowers decreased gradually from F1 to F4 stage, and then increased. The expression level of *FKF1* was lower than that of *GI*. The expression pattern was similar to that of *GI* in leaves, but it fluctuated in pseudobulbs and flowers. With the growth of *Oncidium*, the expression level of *HY5* decreased first and then increased in flowers, pseudobulbs and leaves, and the highest expression levels were found in mature flowers, post-flowering pseudobulbs and young leaves, respectively. *SVP*, an important role in the response of plants to ambient temperature changes, controls flowering time by negatively regulating the expression of a floral integrator, *FT* (*FLOWERING LOCUS T*) (Lee et al., 2007). In *Oncidium*, *SVP* was highly expressed in pseudobulbs and leaves, and lowly expressed in flowers at F1 stage. From vegetative growth to flowering, the expression level of *SVP* increased in pseudobulbs, while the expression level in leaves decreased first and then increased, suggesting that *SVP* functioned mainly in leaves in regulating flowering time. *ICU2* can regulate flowering in vernalization pathway, and its mutants show an early flowering phenotype under both long-day and short-day photoperiod conditions (Hyun et al., 2013). The expression level of *ICU2* in flowers decreased with the flower development, and in vegetative tissues was only detected in young pseudobulbs, which was different from the expression pattern of *ICU2* in *Arabidopsis*. This indicated that *ICU2* had different functions in *Oncidium* that was, it mainly regulated the flower development. *FLK* promotes flowering in the autonomous pathway by negatively regulating the MADS-box floral repressor *FLC* (*FLOWERING LOCUS C*) (Michaels and Amasino, 1999; Lim et al., 2004). In *Oncidium*, *FLK* was expressed in flowers, pseudobulbs and leaves, but the expression patterns were different. The expression level of *FLK* in leaves increased with the growth of *Oncidium*. Its expression level in pseudobulbs increased before flowering, decreased during flowering, and increased after flowering. While in flowers, the expression was increased first and then decreased.

The morphology of floral surfaces depends on the synthesis of cutin (Li-Beisson et al., 2009). Cutin that function is controlled by wax composition, can also block excessive water loss (Kerstiens, 1996; Riederer and Schreiber, 2001). The rich cutin and wax on flower surface of *Oncidiun* may be the reason for the flower shape and long vast life. Cutin, suberin and wax biosynthesis pathway was common enriched in multiple comparisons in this study, indicating that the pathway played a role in the whole process of the flower development in *Oncidium*. In the pathway, *CYP86A1*, *CYP86A4*, *ACE/HTH*, *CER1*, *FAR1* and *FAR4* were screened. Most of them were mainly expressed in flowers, indicating that they played a role in flowers.

Conclusion

In this study, the transcriptome of different tissues from *Oncidium* using RNA-Seq was characterized, and the specific and common DEGs and pathways were identified in flowers. 32 candidate genes related flower development were screened and their expression patterns were analyzed. Among them, 13 MADS-box genes in *Oncidium* were identified, and most of them described by the ABCDE model showed tissue specificity. Phylogenetic analysis result showed that several MADS-box genes were not characterized in previous research. The cutin, suberin and wax biosynthesis pathway was enriched in multiple comparisons, and 11 key genes were obtained in this pathway. In all, these results greatly improve our understanding of the mechanisms underlying the flower development of *Oncidium*. The genes identified in this study could provide valuable

insights into their functions and contribute to understanding the flower development, and probably be applied to in breeding in the future.

Disclaimer: None.
Conflict of Interest: None.
Source of Funding: This research was supported by grants from the Natural Science Foundation of Fujian Province (2020J011371), The Scientific Research Projects of Fujian Academy of Agricultural Sciences (DEC201915), The '5511' Collaborative Innovation Project (XTCXGC2021016) and The Scientific and Technological Innovation Team Construction Project of Fujian Academy of Agricultural Sciences (CXTD2021010-2).

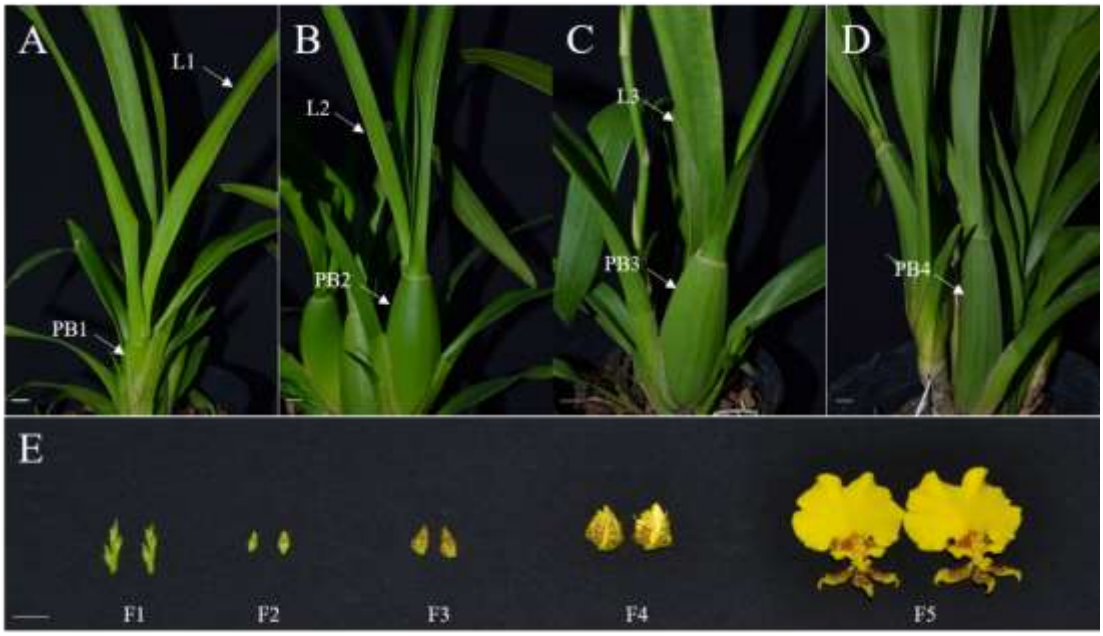

Figure-S1. Samples from *Oncidium* Jinhui were used to transcriptome sequencing. A. The young plant with shoot-pseudobulb in the vegetative stage. B. The mature plant with inflated pseudobulbs. C. The flowering plant. D. The plant after flowering. E. Five development stages of flower. Bar = 1 cm.

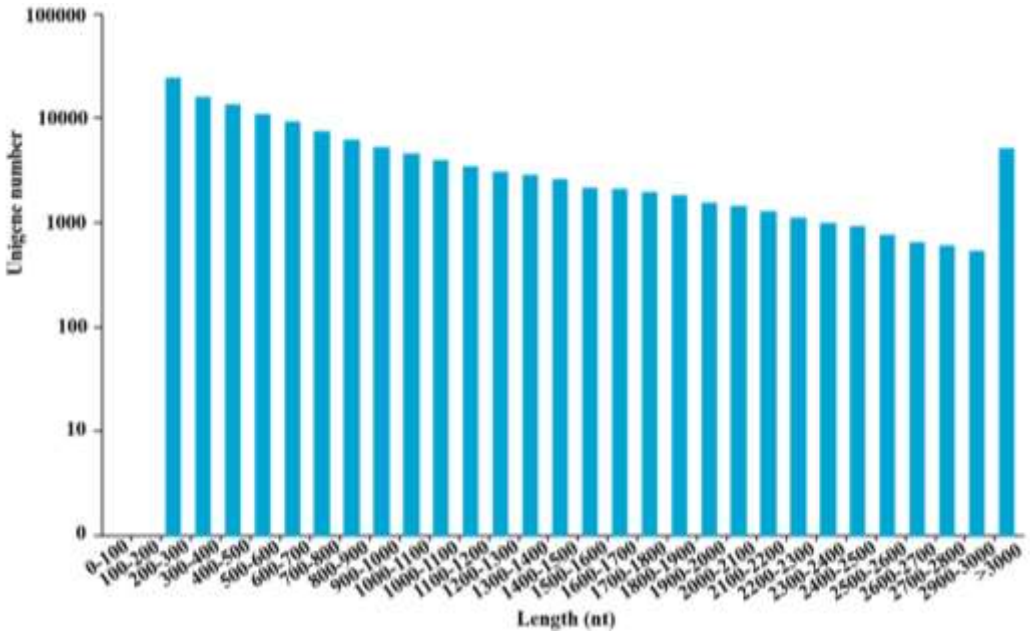

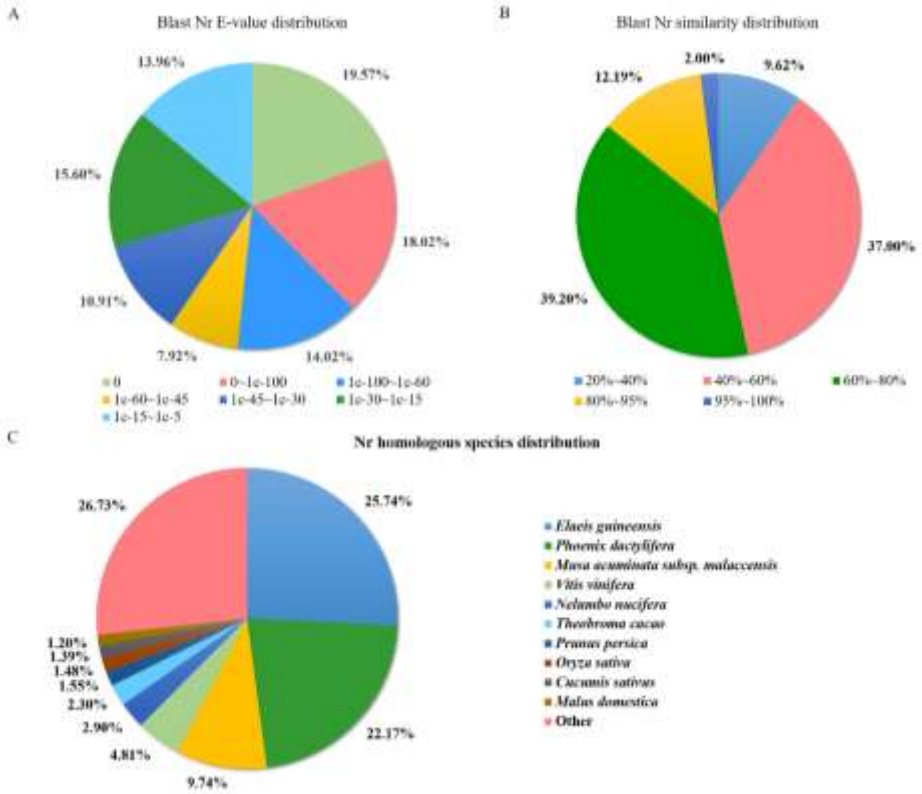

Figure-S2. The length distribution of assembled unigenes from Illumina reads.

Figure-S3. BLAST outputs of unigene sequences against the Nr database. A. The distribution of E-values. B. The distribution of similarity scores. C. The mix of species contributing sequences to the analysis.

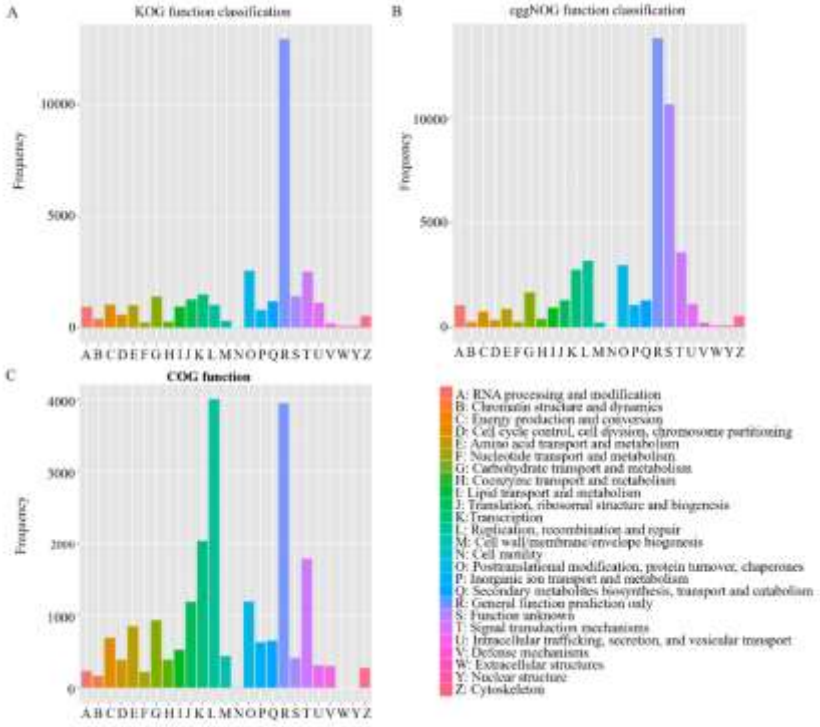

Figure-S4. Unignenes annotation. A. KOG function classification of unigenes; B. COG function classification

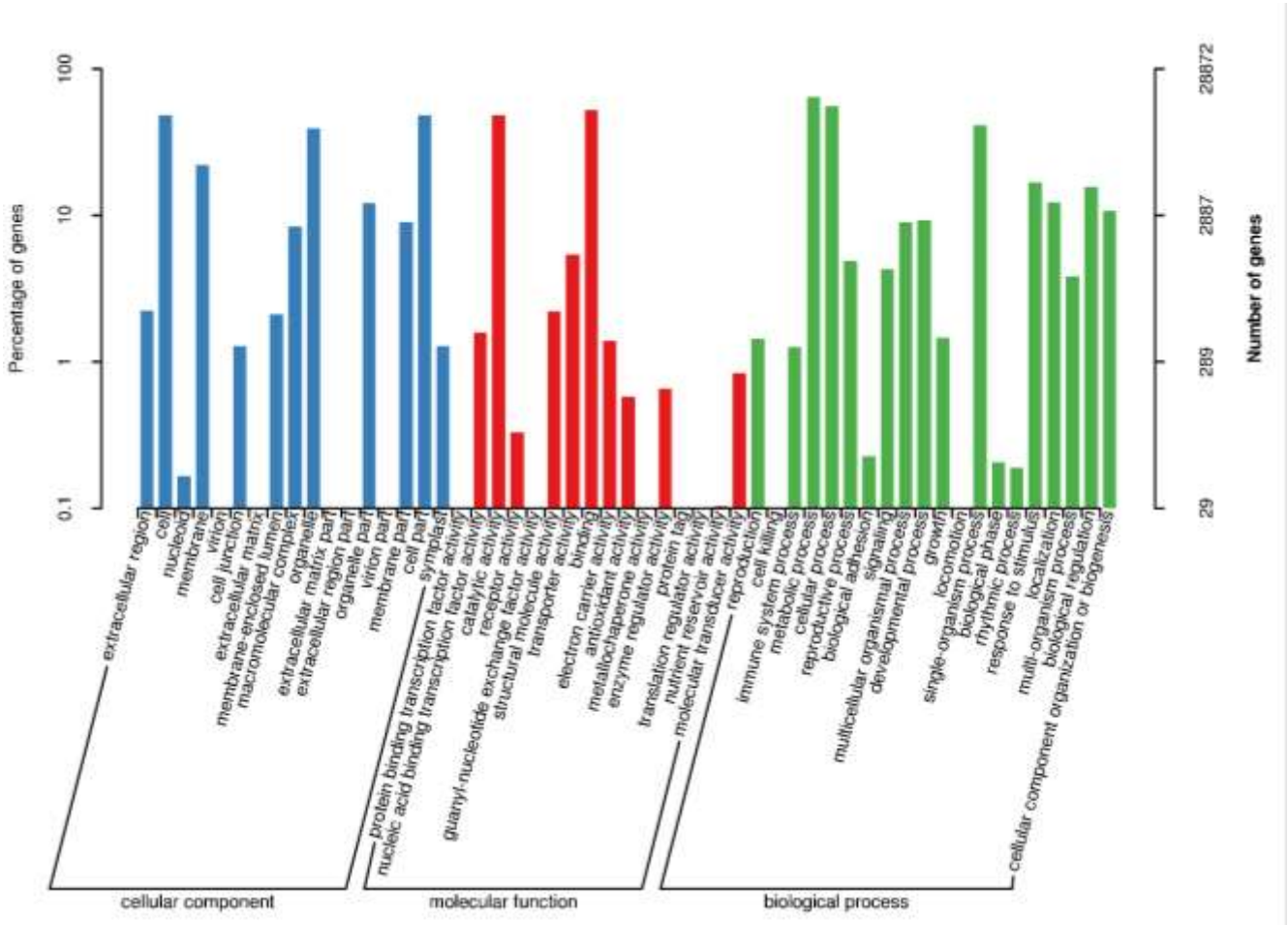

of unigenes; C. eggNOG function classification of unigenes.

Figure-S5. GO function classification of unigenes. The left y-axis indicates the percentage of a specific category of genes in each main category. The right y-axis indicates the number of genes in the same category.

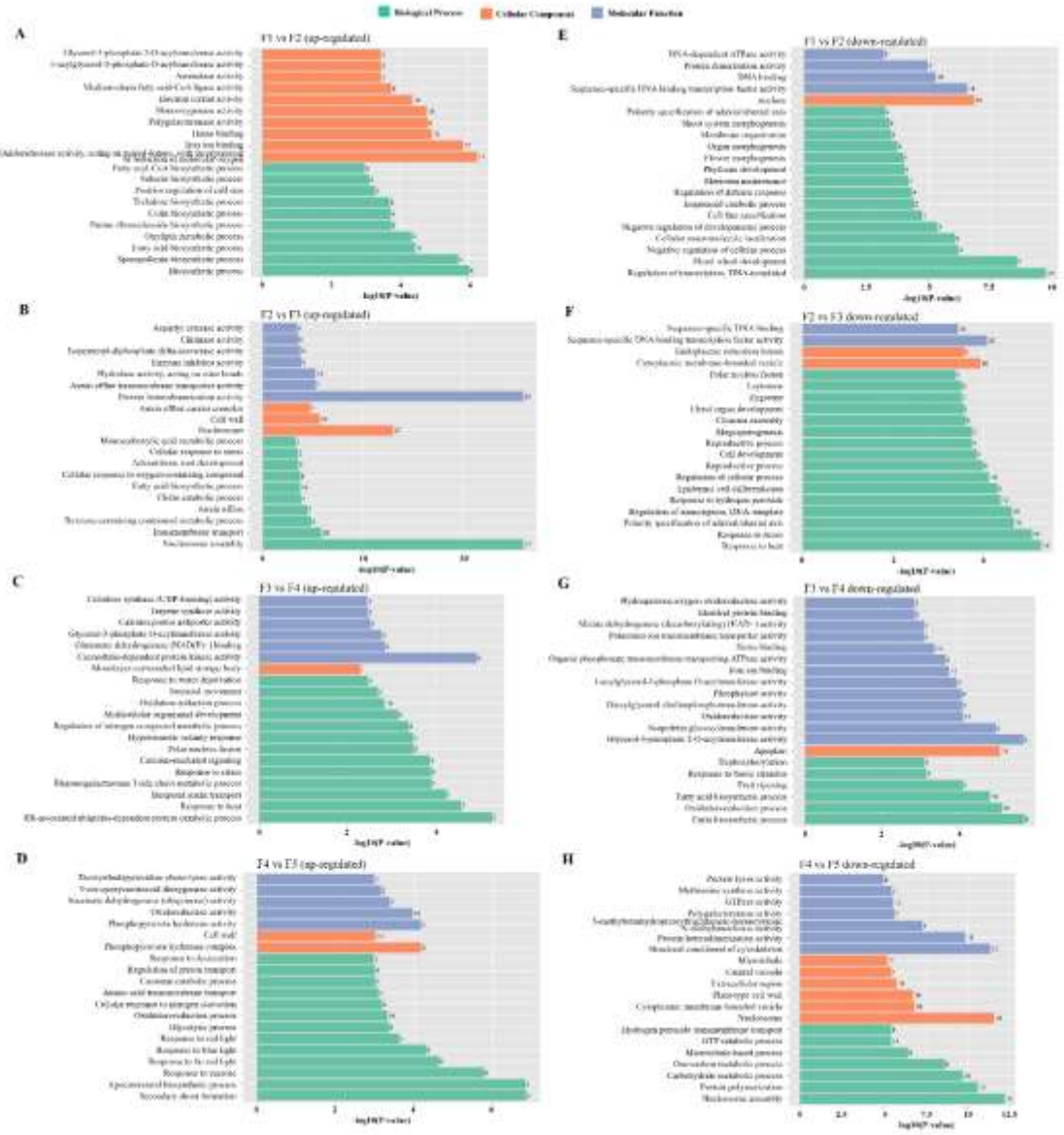

Figure-S6. The most enriched GO terms for specific DEGs in different comparisons. The left y-axis indicates the percentage of a specific category of genes in each main category. The right y-axis indicates the number of genes in the same category.

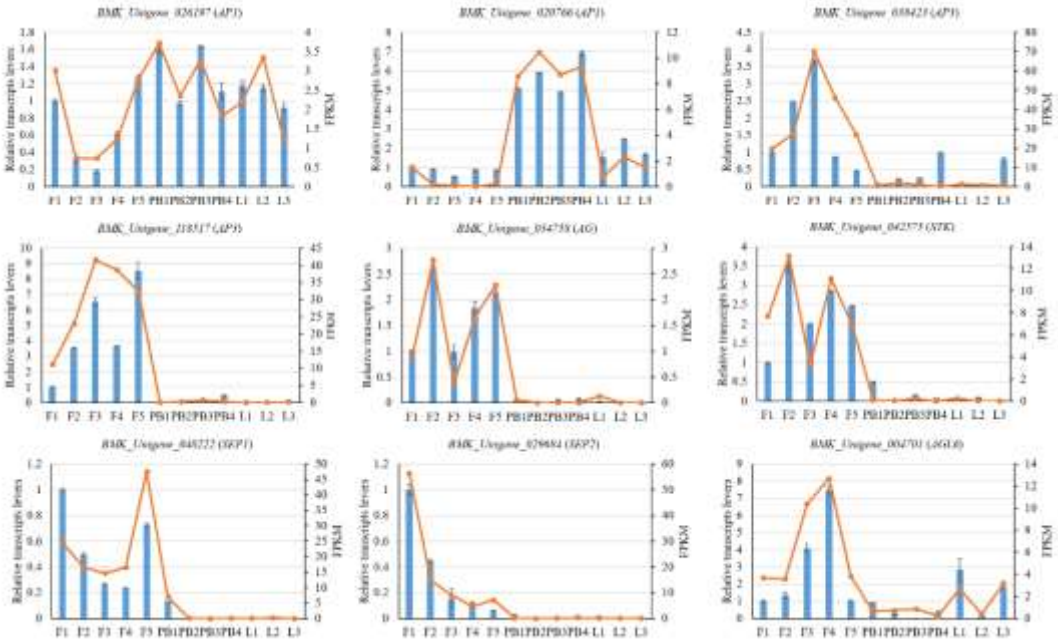

Figure-S7. qRT-PCR validation of nine DEGs selected from the RNA-Seq. The blue bar charts showed the relative expression levels of *AP1*, *AP3*, *AG*, *STK*, *SEP1*, *SEP2*, and *AGL6* genes, respectively, and the line charts showed the corresponding FPKM values of these genes.

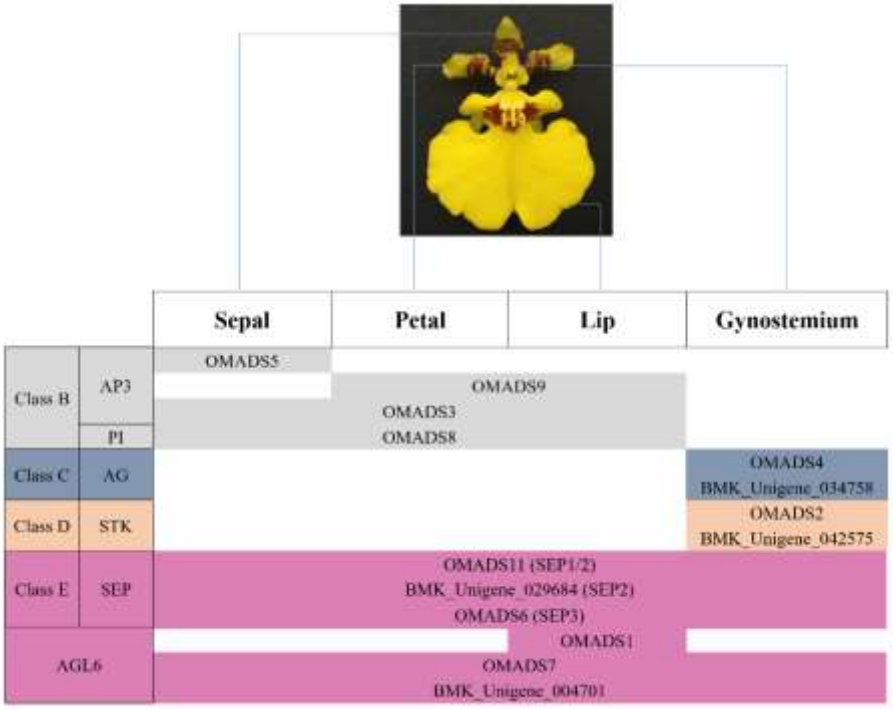

Figure-S8. The pattern of MADS-box genes regulating the flower development of *Oncidium*. E class genes *SEP* and *AGL6* (except for *OMADS1*) regulated sepal, petal, lip and gynostemium development, while *OMADS1* only regulated lip development. C/D class genes *AG* and *STK* only regulated gynostemium development. B class gene *AP3* (*OMADS3*) and *PI* regulated sepal, petal and lip development. *OMADS5* only regulated sepal development, and *OAMDS9* regulated petal and lip development.

Contribution of Authors

Fang N & Zhong H: Conceived idea, designed research methodology, conducted experiments, collected & analyzed data and wrote the manuscript
Luo Y, Fan R & Ye X: Prepared plants and performed q-PCR analysis.
Huang M: Conceived idea, designed research methodology and analyzed data.

References

Altschul SF, Madden TL, Schäffer AA, Zhang J, Miller D and Lipman DJ, 1997. Gapped BLAST and PSI BLAST: A New Generation of Protein Database Search Programs. Nucleic Acids Res. 25(17):3389-3402. https://doi.org/10.1093/nar/25.17.3389.

Anders S and Huber W, 2010. Differential expression analysis for sequence count data. Genome Biology. 11(10):R106. https://doi.org/10.1186/gb-2010-11-10-r106.

Arora R, Agarwal P, Ray S, Singh AK, Singh VP, Tyagi AK and Kapoor S, 2007. MADS-box gene family in rice: genome-wide identification, organization and expression profiling during reproductive development and stress. BMC Genomics. 8(1):242. https://doi.org/0.1186/1471-2164-8-242.

Ashburner M, Ball CA, Blake JA, Botstein D, Butler H, Cherry JM, Davis AP, Dolinski K, Dwight SS, Eppig JT, Harris MA, Hill DP, Issel-Tarver L, Kasarskis A, Lewis S, Matese JC, Richardson JE, Ringwald M, Rubin GM and Sherlock G, 2000. Gene ontology: tool for the unification of biology. The gene ontology consortium. Nature genet. 25(1):25-29. https://doi.org/10.1038/75556.

Callens C, Tucker MR, Zhang D and Wilson ZA, 2018. Dissecting the role of MADS-box genes in monocot floral development and diversity. J Exp Bot. 69(10):2435-2459. https://doi.org/10.1093/jxb/ery086.

Chang YY, Chiu YF, Wu JW and Yang CH, 2009. Four orchid (*Oncidium* Gower Ramsey) *AP1*/*AGL9*-*like* MADS box genes show novel expression patterns and cause different effects on floral transition and formation in *Arabidopsis thaliana*. Plant Cell Physiol. 50(8):1425-1438. https://doi.org/10.1093/pcp/pcp087.

Chang YY, Kao NH, Li JY, Hsu WH, Liang YL, Wu JW and Yang CH, 2010. Characterization of the possible roles for B class MADS box genes in regulation of perianth formation in orchid. Plant Physiol, 152(2):837-853. https://doi.org/10.1104/pp.109.147116.

Chu L, Yang C, Zhuang F, Gao Y and Luo M, 2022. The HDA9-HY5 module epigenetically regulates flowering time in *Arabidopsis thaliana*. J Cell Physiol, 237(7):2961-2968. https://doi.org/10.1002/jcp.30761.

Eddy SR, 1998. Profile hidden Markov models. Bioinformatics. 14(9):755-763. https://doi.org/10.1093/bioinformatics/14.9.755.

Ferrario S, Immink RG and Angenent GC, 2004. Conservation and diversity in flower land. Curr Opin Plant Biol. 7:84-91. https://doi.org/10.1016/j.pbi.2003.11.003.

Finn RD, Bateman A, Clements J, Penelope C, Eberhardt RY, Eddy SR, Andreas H, Kirstie H, Liisa H and Jaina M, 2014. Pfam: the protein families database. Nucleic Acids Res. 42:D222-230. https://doi.org/10.1093/nar/gkt1223.

Givnish TJ, Spalink D, Ames M, Lyon SP, Hunter SJ, Zuluaga A, Iles WJ, Clements MA, Arroyo MT, Leebens-Mack J, Endara L, Kriebel R, Neubig KM, Whitten WM, Williams NH and Cameron KM, 2015. Orchid phylogenomics and multiple drivers of their extraordinary diversification. Proc Biol Sci. 282(1814):20151553. https://doi.org/10.1098/rspb.2015.1553.

Grabherr MG, Haas BJ, Yassour M, Levin JZ, Thompson DA, Amit I, Adiconis X, Fan L, Raychowdhury R, Zeng Q, Chen Z, Mauceli E, Hacohen N, Gnirke A, Rhind N, di Palma F, Birren BW, Nusbaum C, Lindblad-Toh K, Friedman N and Regev A, 2011. Full-length transcriptome assembly from RNA-Seq data without a reference genome. Nature Biotechnol. 29(7):644-652. https://doi.org/10.1038/nbt.1883.

Hew CS, 1992. Orchid cut flower production in Singapore and neighbouring countries. J Am Soc Hort Sci. 27(6):887-898. https://doi.org/10.21273/HORTSCI.27.6.609c.

Huerta-Cepas J, Szklarczyk D, Forslund K, Cook H, Heller D, Walter MC, Rattei T, Mende DR, Sunagawa S, Kuhn M, Jensen LJ, von Mering C and Bork P, 2016. eggNOG 4.5: a hierarchical

orthology framework with improved functional annotations for eukaryotic, prokaryotic and viral sequences. Nucleic Acids Res. 44(D1):D286-D293. https://doi.org/10.1093/nar/gkv1248.

Hsu HF and Yang CH, 2002. An orchid (*Oncidium* Gower Ramsey) *AP3-like* MADS gene regulates floral formation and initiation. Plant Cell Physiol. 43(10):1198-1209. https://doi.org/10.1093/pcp/pcf143.

Hsu HF, Huang CH, Chou LT and Yang CH, 2003. Ectopic expression of an orchid (*Oncidium* Gower Ramsey) *AGL6-like* gene promotes flowering by activating flowering time genes in *Arabidopsis thaliana*. Plant Cell Physiol. 44(8):783-794. https://doi.org/10.1093/pcp/pcg099.

Hsu HF, Hsieh WP, Chen MK, Chang YY and Yang CH, 2010. C/D class MADS box genes from two monocots, orchid (*Oncidium* Gower Ramsey) and lily (*Lilium longiflorum*), exhibit different effects on floral transition and formation in *Arabidopsis thaliana*. Plant Cell Physiol. 51(6):1029-1045. https://doi.org/10.1093/pcp/pcq052.

Hyun Y, Yun H, Park K, Ohr H, Lee O, Kim DH, Sung S and Choi Y, 2013. The catalytic subunit of *Arabidopsis* DNA polymerase α ensures sTable - maintenance of histone modification. Development. 140(1):156-66. https://doi.org/10.1242/dev.084624.

Kanehisa M, Goto S, Kawashima S, Okuno Y and Hattori M, 2004. The KEGG resource for deciphering the genome. Nucleic Acids Res. 32:D277-280. https://doi.org/10.1093/nar/gkh063.

Imaizumi T, Schultz TF, Harmon FG, Ho LA and Kay SA, 2005. FKF1 F-box protein mediates cyclic degradation of a repressor of CONSTANS in *Arabidopsis*. Science. 309:293-297. https://doi.org/10.1126/SCIENCE.1110586.

Kerstiens G, 1996. Cuticular water permeability and its physiological significance. J Exp Bot. 47(305):1813-1832. https://doi.org/10.1093/jxb/47.12.1813.

Koonin EV, Fedorova ND, Jackson JD, Jackson JD, Jacobs AR, Krylov DM, Makarova KS, Mazumder J, Mekhedov SL, Nikolskaya AN, Rao BS, Rogozin IB, Smirnov S, Sorokin AV, Sverdlov AV, Vasudevan S, Wolf YI, Yin JJ and Natale DA, 2004. A comprehensive evolutionary classification of proteins encoded in complete eukaryotic genomes. Genome Biol. 5(2):R7. https://doi.org/10.1186/gb-2004-5-2-r7.

Langmead B, Trapnell C, Pop M and Salzberg SL, 2009. Ultrafast and memory-efficient alignment of short DNA sequences to the human genome. Genome Biology. 10(3):R25. https://doi.org/10.1186/gb-2009-10-3-r25.

Michaels SD and Amasino RM, 1999. *FLOWERING LOCUS C* encodes a novel MADS domain protein that acts as a repressor of flowering. Plant Cell. 11(5):949-56. https://doi.org/10.1105/tpc.11.5.949.

Lee JH, Yoo SJ, Park SH, Hwang I, Lee JS and Ahn JH, 2007. Role of SVP in the control of flowering time by ambient temperature in *Arabidopsis*. Genes Dev. 15;21(4):397-402. https://doi.org 10.1101/gad.1518407.

Leitch IJ, Kahandawala I, Suda J, Hanson L, Ingrouille MJ, Chase MW and Fay MF, 2009. Genome size diversity in orchids: consequences and evolution. Ann Bot. 104(3):469-481. https://doi.org/10.1093/aob/mcp003.

Li B and Dewen CN, 2011. RSEM: accurate transcript quantification from RNA Seq data with or without a reference genome. BMC Bioinformatics, 12(1):323. https://doi.org/10.1186/1471-2105-12-323.

Li-Beisson Y, Pollard M, Sauveplane V, Pinot F, Ohlrogge J and Beisson F, 2009. Nanoridges that characterize the surface morphology of flowers require the synthesis of cutin polyester. Proc Natl Acad Sci U S A. 106(51):22008-22013. https://doi.org/10.1073/pnas.0909090106.

Lim MH, Kim J, Kim YS, Chung KS, Seo YH, Lee I, Kim J, Hong CB, Kim HJ and Park CM, 2004. A new *Arabidopsis* gene, *FLK*, encodes an RNA binding protein with K homology motifs and regulates flowering time via *FLOWERING LOCUS C*. Plant Cell. 16(3):731-40. https://doi.org/doi: 10.1105/tpc.019331.

Livak KJ and Schmittgen TD, 2001. Analysis of relative gene expression data using real-time quantitative PCR and the 2(-Delta Delta C(T)) Method. Methods. 25(4):402-408. https://doi.org/10.1006/meth.2001.1262.

Mandel MA, Gustafson-Brown C, Savidge B and Yanofsky MF, 1992. Molecular

characterization of the *Arabidopsis* floral homeotic gene *APETALA1*. Nature. 360(6401):273-277. https://doi.org/10.1038/360273a0.

Marioni JC, Mason CE, Mane SM, Stephens M and Gilad Y, 2008. RNA-seq: an assessment of technical reproducibility and comparison with gene expression arrays. Genome Res. 18(9):1509-1517. https://doi.org/10.1101/gr.079558.108.

Riederer M and Schreiber L, 2001. Protecting against water loss: analysis of the barrier properties of plant cuticles. J Exp Bot. 52(363):2023-2032. https://doi.org/10.1093/jexbot/52.363.2023.

Sawa M, Nusinow DA, Kay SA and Imaizumi T, 2007. FKF1 and GIGANTEA complex formation is required for day-length measurement in *Arabidopsis*. Science. 318:261-265. https://doi.org/10.1126/SCIENCE.1146994.

Tatusov RL, Galperin MY, Natale DA and Koonin EV, 2000. The COG database: a tool for genome-scale analysis of protein functions and evolution. Nucleic Acids Res. 28(1):33-36. https://doi.org/10.1093/nar/28.1.33.

The UniProt Consortium, 2018. UniProt: the universal protein knowledgebase. Nucleic Acids Res. 46(5):2699. https://doi.org/10.1093/nar/gky092.

Theissen G, 2001. Development of floral organ identity: stories from the MADS house. Curr Opin Plant Biol. 4(1):75-85. https://doi.org/10.1016/s1369-5266(00)00139-4.

Weigel D and Meyerowitz EM, 1994. The ABCs of floral homeotic genes. Cell. 78(2):203-209. https://doi.org/10.1016/0092-8674(94)90291-7.

Xie C, Mao X, Huang J, Ding Y, Wu J, Dong S, Kong L, Gao G, Li CY and Wei L, 2011. KOBAS 2.0: a web server for annotation and identification of enriched pathways and diseases. Nucleic Acids Res. 39:W316-322. https://doi.org/10.1093/nar/gkr483.

Yanofsky MF, Ma H, Bowman JL, Drews GN, Feldmann KA and Meyerowitz EM, 1990. The protein encoded by the *Arabidopsis* homeotic gene agamous resembles transcription factors. Nature. 346(6279):35-39. https://doi.org/10.1038/346035a0.